Abdominal Radiology


Published online: 8 November 2018

Abdom Radiol (2019) 44:1340–1349
https://doi.org/10.1007/s00261-018-1812-9

# Assessing liver function: diagnostic efficacy of parenchymal enhancement and liver volume ratio of Gd-EOB-DTPA-enhanced MRI study during interstitial and hepatobiliary phase

Davide Ippolito,[1,2] Anna Pecorelli,[1,2] Simone Famularo,[1,3] Davide Bernasconi,[4] Eleonora Benedetta Orsini,[1,2] Alessandro Giani,[1,3] Fabrizio Romano,[1,3] Cammillo Talei Franzesi,[1,2] and Sandro Sironi[5,6]

[1]School of Medicine, University of Milano-Bicocca, Milan, Italy
[2]Department of Diagnostic Radiology, H. S. Gerardo Monza, Via Pergolesi 33, 20900 Monza, MB, Italy
[3]Department of Surgery, H. S. Gerardo Monza, Via Pergolesi 33, 20900 Monza, MB, Italy
[4]Center of Biostatistics for Clinical Epidemiology, Department of Health Sciences, University Milano-Bicocca, Monza, Italy
[5]Department of Radiology, ASST Papa Giovanni XXIII, Bergamo, Italy
[6]University of Milano-Bicocca, Milan, Italy

## Abstract

*Aim:* To assess the efficacy of signal intensity in interstitial and hepatobiliary phase normalized for liver volume, on gadolinium-ethoxybenzyl-diethylenetriaminepentaacetic acid (Gd-EOB-DTPA)-enhanced magnetic resonance imaging (MRI) study, for the evaluation of liver function through the comparison with Child–Pugh (CP), model for end-stage liver disease (MELD), and biochemical tests.

*Methods:* All dynamic Gd-EOB-DTPA MRI studies performed in patients with suspected liver lesions were retrospectively reviewed. The rate of liver-to-muscle ratio on T1 sequence 70 s (interstitial phase) and 20 min (hepatobiliary phase) after injection of Gd-EOB-DTPA was calculated for each MRI study and then normalized for liver volume (irINTnorm and irHEPnorm). Pearson correlation coefficient was computed to assess the correlation among these values and CP and MELD scores, and biochemical tests.

*Results:* A total of 303 MRI studies, performed on 221 patients, were included. Mean age was 63.8 years ± 12.9 with a majority of male patients (186; 61.4%). A total of 186 out of 303 (61.4%) were cirrhotic patients. The irHEPnorm was significantly lower in cirrhotic than non-cirrhotic patients (0.0004 ± 0.0002 to 0.0005 ± 0.0003, $p = 0.010$). This value had a moderate, significant correlation with Child–Pugh and MELD scores ($R = -0.292$, $p < 0.0001$ and $R = -0.192$, $p = 0.010$, respectively). In particular, irHEPnorm progressively decreased from Child–Pugh A to C (0.0004–0.0002, $p < 0.0001$) and from MELD ≤ 10 to 19–24 (0.0004–0.0003, $p = 0.018$). Among biochemical parameters, total bilirubin, GOT, and albumin had the strongest correlation with irHEPnorm ($R = -0.258$, $-0.291$, and 0.262, $p < 0.0001$, respectively). No correlations were found between irINTnorm and CP and MELD scores.

*Conclusion:* irHEPnorm value derived from Gd-EOB-DTPA-enhanced MRI is a reliable, non-invasive, useful tool to quantify liver function and to assess the degree of cirrhosis, offering a strict relationship with clinical scores and biochemical parameters. This could help surgeons in clinical decision-making, allowing them to choose the more suitable surgical approach for cirrhotic patients.

**Key words:** Magnetic resonance—Cirrhosis—Surgery—Liver

The proper characterization of unknown focal liver lesions is mandatory to define the therapeutic management or, eventually, follow-up of patients. When a surgical approach is considered feasible, the assessment of liver function is pivotal, especially in patients with liver dis-

*Correspondence to:* Davide Ippolito; *email:* davide.atena@tiscalinet.it

ease, since it defines the risk of post-hepatectomy liver failure.

In daily clinical practice, liver function is usually evaluated through biochemical parameters combined together to create clinical scores. Child–Pugh and MELD scores reflect the liver functional reserve better than the biochemical parameters alone and are routinely used in clinical practice [1]. Several non-invasive techniques able to evaluate liver function have been used in the literature: indocyanine green (ICG) clearance test, Technetium-99m galactosyl serum albumin (99mTc-GSA) scintigraphy, 99m Tc-labeled mebrofenin scintigraphy, computed tomography (CT), and magnetic resonance imaging (MRI)-based techniques [2–5]. The estimation of liver volume, with CT or MRI post-processing analysis, is particularly useful in the surgical setting to estimate the remnant liver volume and the risk of acute liver failure after surgery. In fact, it is demonstrated that liver volume well correlates with liver function in cirrhotic patients and in acute liver failure [5]. In particular, a significant correlation has been found between liver volume index calculated on MRI and the severity of liver cirrhosis [6]. Furthermore, MRI plays an increasing key role not only in the estimation of liver volume but also in the follow-up of cirrhotic patients, as well as in the diagnostic algorithm of non-cirrhotic patients with unknown focal liver lesion. In fact, due to the employment of hepatobiliary intravenous contrast agents, it has shown a high capability in detecting and characterizing focal liver lesions.

Gadolinium-ethoxybenzyl-dimeglumine (Gd-EOB-DTPA; Primovist®, Bayer Healthcare, Berlin) is a paramagnetic contrast agent for T1-weighted imaging. After intravenous injection, approximately 50% of the injected dose undergoes specific OATP1B1/B3-dependent hepatocyte uptake and, then, it is excreted in the biliary drainage system through MDRP2 without metabolic changes. For this reason, it is supposed to directly reflect the hepatocyte function. In the last years, many authors described the relationship between parenchymal signal intensity and liver function by means of Child–Pugh and MELD scores, ICG test, or liver fibrosis, using different function indices [7–13], but the value of signal intensity on T1 sequences normalized for liver volume has been poorly investigated and mainly through a comparison with ICG or 99mTc-GSA scintigraphy [14–16]. Moreover, due to the pharmacodynamics properties of Gd-EOB-DTPA, all these studies focused only on the signal intensity during the hepatobiliary phase. However, this contrast media has also a vascular and extravascular distribution during the standard dynamic phases and the highest signal intensity is detectable during the early interstitial phase [17]. For this reason, the aim of our study was to evaluate the diagnostic efficacy of signal intensity both in interstitial and hepatobiliary phase normalized for liver volume, through Gd-EOB-DTPA-enhanced MRI studies using a correlation with clinical scores and biochemical parameters, as reference standard.

## Materials and methods

A total of 618 MRI liver studies for the characterization of focal liver lesions were performed between May 2010 and September 2016 at our institution and retrospectively reviewed.

All data of this retrospective study were obtained from consecutive routine clinical examinations. The institutional review board approved this study with a waiver for informed patient consent.

Patients were eligible for study inclusion if they were (1) suspected of having focal hepatic lesions according to previously performed ultrasonography or CT; (2) scheduled to undergo or previously underwent (within ≤ 1 months from MRI studies) biochemical liver function tests; (3) not pregnant; (4) at least 20 years of age.

Exclusion criteria were (1) use of other MRI contrast agent, different from Gd-EOB-DTPA; (2) history of previous hepatic treatment such as liver surgery, percutaneous ethanol injection (PEI), radiofrequency ablation (RA), transarterial chemoembolization (TACE) or selective internal radiation therapy (SIRT); (3) history of anaphylactic reaction to liver-specific MRI contrast media; (4) renal failure (defined as estimated glomerular filtration rate $> 30$ mL/min/1.73 $m^2$); (5) contraindication to MRI (e.g., non-compatible biometallic implants or claustrophobia).

Therefore, only 303 out of the 618 eligible patients met the above-mentioned inclusion and exclusion criteria (Fig. 1).

Patients were divided into study and control group according to the presence or absence of liver cirrhosis. The diagnosis of cirrhosis was based on histology in 70 patients. In the remaining cases, cirrhosis was diagnosed according to international guidelines released during the study period and on the basis of unequivocal laboratory exams and radiological findings (i.e., hypertrophy of caudate and left lobe, irregular liver burden, coarse parenchymal pattern) [18].

### *Image technique*

All patients underwent an upper abdominal examination on a 1.5 T Magnet (Achieva Plus, Philips, The Netherlands), using a 16-channel phased-array body coil. The standard liver imaging protocol included axial T1-weighted in- and out-of-phase breath-hold spoiled gradient-echo (GE) sequences, axial turbo spin-echo T2-weighted, respiratory-triggered and also fat-suppressed sequences, diffusion-weighted-images (DWI), and axial 3D T1-weighted fat-suppressed spoiled recalled-echo sequences (THRIVE). The dynamic images were obtained

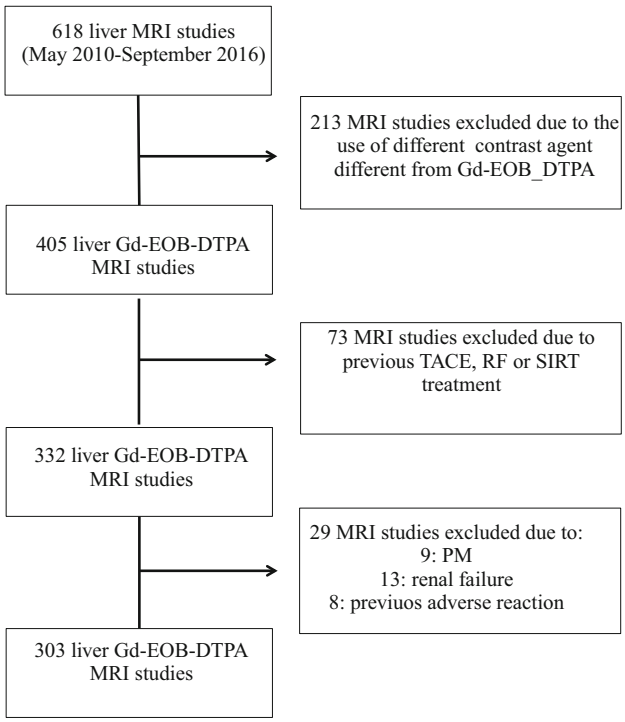


**Fig. 1.** Flow diagram of the study.

before and after intravenous injection of 0.1 mL/kg of Gd-EOB-DTPA, with a flow rate of 1 mL/s and followed by a 30-mL saline flush at the same rate, using a power injector (The Medrad®Stellant®) and acquiring three different contrastographic phases (arterial, interstitial, and delayed). A real-time display, using fluoroscopic technique, returned low-resolution images every second to permit breath-hold coordination with contrast arrival at the level of the celiac trunk, in order to acquire the arterial phase of hepatic enhancement. The interstitial and delayed phases were acquired after 70 and 140 s, respectively, from the injection of contrast media. Hepatocyte-phase images were obtained 20 min after contrast agent administration

Sequences parameters used for DCE-MRI liver protocol are shown in Table 1.

## *Image analysis*

MRI studies were provided on a dedicated workstation (Agfa, Belgium). The mean signal intensity values of liver parenchyma and paravertebral muscle were measured on pre-contrast, 70-s delayed, and 20-min delayed Gd-EOB-DTPA-enhanced T1-weighted images using operator-defined region-of-interest (ROI) methods. Three ROIs (2 in right lobe, 1 in left lobe) were drawn in liver parenchyma and one ROI was located in the paravertebral muscle.

A single radiologist, with 10 years' experience in liver imaging and Gd-EOB-DTPA imaging, outlined each ROI, which was drawn as large as possible avoiding the inclusion of confounding structures such as blood vessels, artifacts, or focal liver lesions.

Liver volume was calculated on hepatobiliary phase, which is the phase with the highest signal intensity, with free-hand contours using a dedicated software (Intellispace Portal, Philips, The Netherlands).

To quantify the enhancement in interstitial (INT) and hepatobiliary (HEP) phase, respectively, we calculated the relative liver-to-muscle ratio, comparing the mean value of signal intensity of ROI drawn in the liver and muscles, in both different phases using the following formula (Figs. 2 and 3):

$$\text{irINT} = \frac{(\text{icINTl}/\text{icINTm}) - (\text{icBASl}/\text{icBASm})}{(\text{icBASl}/\text{icBASm})}$$

$$\text{irHB} = \frac{(\text{icHBl}/\text{icHBm}) - (\text{icBASl}/\text{icBASm})}{(\text{icBASl}/\text{icBASm})},$$

where l represents the liver and m represents the muscle.

For the purpose of this study, we chose this formula since paravertebral muscles are generally considered the reference standard for the signal intensity in MRI, and in fact in comparison to other parenchyma such as the spleen they have a more homogeneous enhancement [14].

Subsequently, the obtained values were then normalized for liver volume (Figs. 2 and 3):

$$\text{irINTnorm} = \text{irINT}/\text{liver volume}$$

$$\text{irHBnorm} = \text{irHB}/\text{liver volume}.$$

## *Biochemical tests and liver function*

Patients' biochemical tests inclusive of albumin, total bilirubin, direct bilirubin, prothrombin time (PT), International Normalized Ratio (INR), Glutamic Oxaloacetic Transaminase (GOT), Glutamic Pyruvate Transaminase (GPT), Gamma Glutamyl Transferase (GGT), Alkaline Phosphatase (ALP), sodium, and creatinine were reviewed and recorded.

Hepatic function was assessed through Child–Pugh and MELD scores in patients with known liver disease or clinical and radiological signs of liver disease.

Child–Pugh score was obtained by the sum of INR (1 point, $< 1.7$; 2 points, 1.71–2.3; 3 points, $> 2.3$), serum albumin (g/dl, 1 point, $> 3.5$; 2 points, 2.8–3.5; 3 points, $< 2.8$), serum bilirubin (mg/dl, 1 point, $< 2$; 2 points, 2–3; 3 points, $> 3$), ascites (1 point, none; 2 points, mild; 3 points, moderate to severe), and encephalopathy (1 point, none; 2 points, Grade I–II; 3 points, Grade III–IV)[19].

MELD score was derived by the formula: 3.78 [Ln bilirubin] + 11.2 [Ln INR] + 9.57 [Ln creatinine] + 6.43 [20].

**Table 1.** Descriptive parameters of acquisition protocol for the study of upper abdomen employed

| Sequences | Acquisition parameters | | | | | |
|---|---|---|---|---|---|---|
| | FA (°) | Thickness (mm) | TR (ms) | TE (ms) | NSA | Matrix size |
| T1 in-phase ax | 80 | 5 | 181 | 2.30 | 1 | 192 × 114 |
| T1 out-phase ax | 80 | 5 | 181 | 4.60 | 1 | 192 × 114 |
| T2 TSE SPAIR ax (respiratory triggered) | 90 | 5 | 432 | 80 | 2 | 236 × 174 |
| T2 TSE ax | 90 | 5 | 522 | 80 | 2 | 268 × 240 |
| THRIVE ax (4 dynamic phases) | 15 | 2 | 4.1 | 1.97 | 2 | 176 × 160 |
| THRIVE cor | 15 | 2 | 4.1 | 1.97 | 2 | 188 × 188 |
| DWI | 90 | 5 | 63 | 1.89 | 2 | 124 × 105 |

FA, flip angle; TR, repetition time; TE, echo time; NSA, number of signal acquired; AX, axial plane; COR, coronal plane; DWI, diffusion-weighted images

### *Statistical analysis*

Continuous variables were expressed as mean ± standard deviation (SD) and categorical variables as number of cases and proportions. Variable distribution was assessed by the Kolmogorov–Smirnov test, and continuous variables were compared using Student *t* test or the analysis of variance (ANOVA) as appropriate.

The correlation between irHEPnorm or irINTnorm and Child–Pugh, MELD score, and biochemical parameters was calculated with Pearson coefficient.

The prognostic accuracy of irHEPnorm or irINTnorm was assessed through the calculation of the areas under the receiver operator curve (AUROC), where values close to 1.0 indicate an ideal parameter and values below 0.5 indicate a parameter without prognostic significance. Confidence intervals at 95% (95% CI) are shown as well. The best cut-off for each parameter was chosen to maximize sensitivity and specificity.

A two-tailed $p < 0.05$ was considered statistically significant. All statistical analyses were performed using the SPSS 21.0 statistical package (SPSS Incorporated, Chicago, Illinois, USA).

## Results

A total of 303 consecutive Gd-EOB-DTPA-enhanced MRI studies, performed in 221 consecutive patients, were included in the study. The majority of patients were male (186 [61.4%]) and mean age was 63.8 ± 12.9 years, ranging from 55 to 74 years.

One hundred eighty-six [61.4%] Gd-EOBDTPA-enhanced MRI studies were performed on cirrhotic patients, of whom 116 [62.3%] were radiologically detectable.

Thirty-nine patients, of whom 31 in the whole cirrhotic group, performed more than one MRI study. For each MRI study, new blood tests and clinical assessments were performed.

Among cirrhotic patients, the median Child–Pugh score was 5 (IQR 5–6); 153 (81.8%) patients belonged to class A, 24 (12.9%) to class B, and 9 (4.8%) to class C.

The median MELD score value was 8.75 (IQR 6.76–11.05); 116 patients had a score ≤ 10, 64 (34.4%) between 11 and 18, and 6 (3.3) between 19 and 24 (Table 2).

## Interstitial and hepatobiliary rate of liver-to-muscle ratio normalized for liver volume in cirrhotic and non-cirrhotic patients

The mean liver-to-muscle ratios in interstitial and hepatobiliary phase were 0.34 (± 0.21) and 0.59 (± 0.34), respectively. The mean liver volume was 1426 (± 374.4). Table 3 summarizes the values of rate of liver-to-muscle ratio normalized for liver volume in cirrhotic and non-cirrhotic groups and in Child–Pugh (A, B, and C) and MELD classes (≤ 10, 11–18, 19–24).

The irHEPnorm was significantly lower in cirrhotic than non-cirrhotic patients (0.0004 ± 0.0002 vs. 0.0005 ± 0.0003, $p = 0.010$), while no differences were found in irINTnorm (Table 3, Fig. 4).

## Association between liver function and rate of liver-to-muscle ratio normalized for liver volume

### *Association with Child–Pugh score*

A significant, moderate, and negative correlation was found between Child–Pugh score and irHEPnorm ($R = -0.292$ $p < 0.0001$), while no correlation was found between Child–Pugh (score and class) and irINTnorm (Table 4).

The irHEPnorm progressively and significantly decreases with the worsening of liver function, from Child–Pugh A to Child–Pugh C (from 0.0004 ± 0.0002 to 0.0002 ± 0.0002, $p < 0.0001$) (Fig. 4).

Through the dynamic phase, the rate of liver-to-muscle ratio normalized for LV significantly increased from interstitial to hepatobiliary phase in non-cirrhotic (from 0.0002 ± 0.0001 to 0.0005 ± 0.0003, $p < 0.0001$) and in Child–Pugh A patients (from 0.0003 ± 0.0002 to 0.0004 ± 0.0002, $p < 0.0001$). Instead, in Child–Pugh C patients the rate of liver-to-muscle ratio normalized for

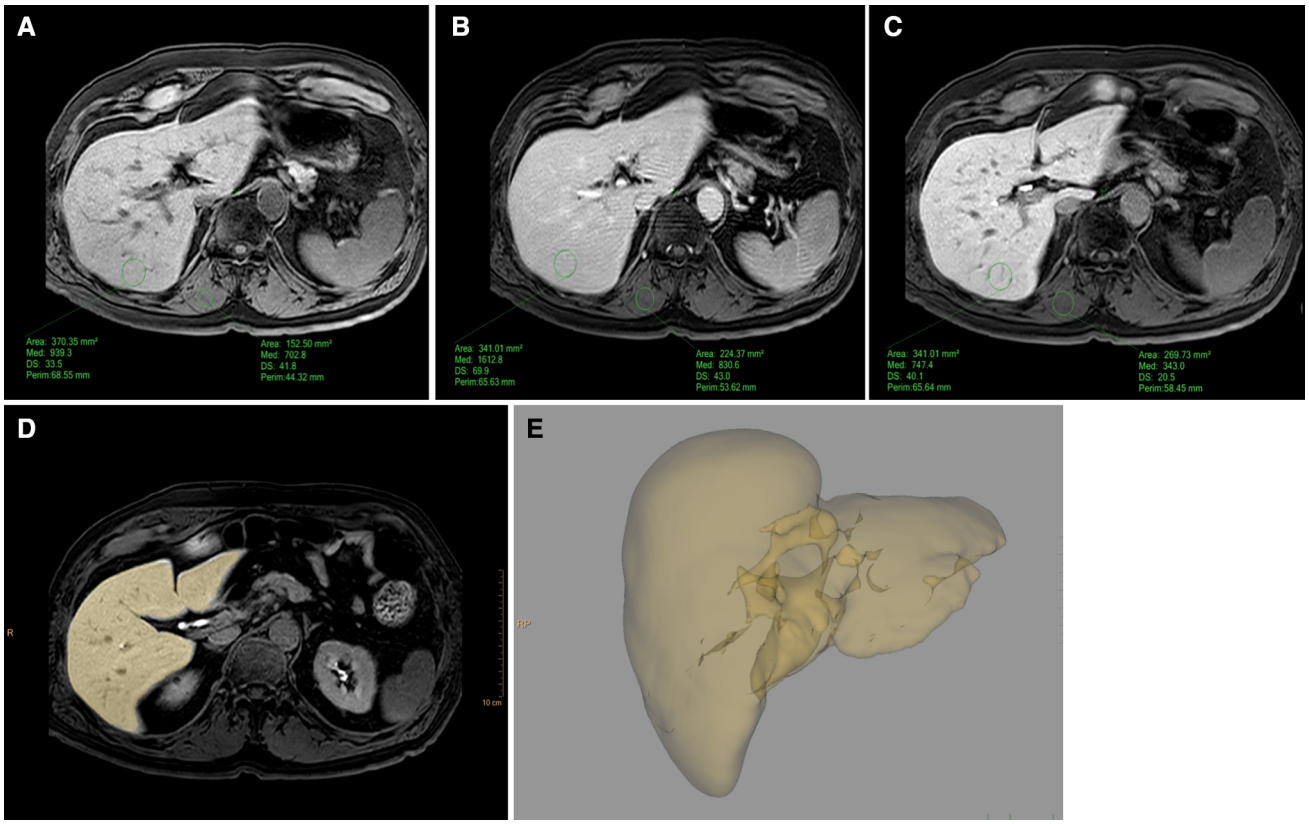


**Fig. 2.** A 69-year-old man, with focal lesion in a non-cirrhotic liver. Panels **A**, **B,** and **C**: axial unenhanced, 70-s delayed, and 20-min delayed Gd-EOB-DTPA-enhanced T1-weighted images with operator-defined region-of-interest (ROI) drawn on the left liver lobe and on the right paravertebral muscle. Panels **D** and **E**: liver volume calculated on hepatobiliary phase with free-hand contours using dedicated software (Intellispace Portal, Philips, The Netherlands).

LV decreased from interstitial to hepatobiliary phase, however without a statistically significant difference (from $0.0003 \pm 0.0002$ to $0.0003 \pm 0.0002$, $p = 0.305$) (Table 3).

No modification was observed in Child–Pugh B patients, (from $0.0003 \pm 0.0002$ to $0.0003 \pm 0.0002$, $p = 1$) (Table 3).

### *Association with MELD score*

A significant, moderate, and negative correlation was also found between MELD score and irHEPnorm ($R = -0.192$, $p = 0.010$). No correlations were found between MELD (score and class) and the irINTnorm (Table 3).

The irHEPnorm progressively decreases from MELD class ≤ 10 to 19–24 ($0.0004 \pm 0.0002$ to $0.0002 \pm 0.0002$, $p = 0.018$) (Fig. 4).

The signal intensity normalized for liver volume significantly increased from interstitial to hepatobiliary phase only in MELD class ≤ 10 (from $0.0003 \pm 0.0002$ to $0.0004 \pm 0.0002$, $p = 0.0002$), while in MELD class 11–18 and 19–24 a slight increase was observed, however without a statistically significant difference (Table 3).

## Association between biochemical parameters and the rate of liver-to-muscle ratio normalized for liver volume

Mean (± SD) of biochemical variables are summarized in Table 4.

Among the biochemical parameters analyzed, total bilirubin, GOT, and albumin had the strongest, although moderate correlation with the rate of liver-to-muscle ratio normalized for liver volume in hepatobiliary phase ($R = -0.258$, $-0.291$, and $0.262$). No correlation was found among biochemical parameters and irINTnorm (Table 5).

## ROC analysis

The hepatobiliary enhancement normalized for liver volume had a good performance in the evaluation of liver function (Fig. 5). In particular, a cut-off value of 0.262 showed good sensitivity and specificity (78.3% and 67.6%, respectively) in discriminating Child–Pugh A vs. B and C patients, with an AUROC of 0.733 (0.650–0.815 95% CI). The more accurate value in discriminating a MELD score ≤ 10 and > 10 was 0.317 with good sen-

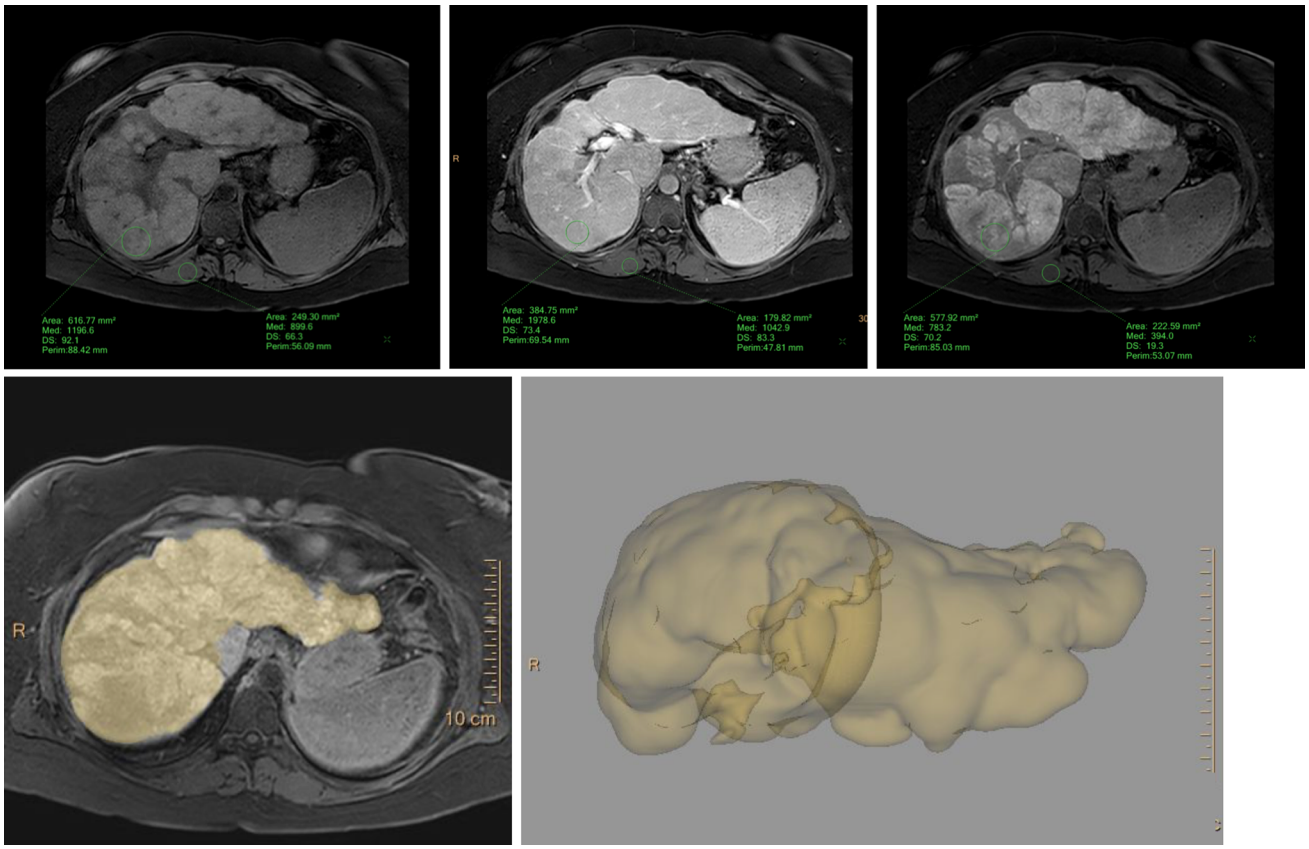


**Fig. 3.** A 57-year-old woman, with cirrhosis and a suspected focal liver lesion. Panels **A**, **B**, and **C**: axial pre-contrast, 70-s delayed, and 20-min delayed Gd-EOB-DTPA-enhanced T1-weighted images with operator-defined region-of-interest (ROI) drawn on the left liver lobe and on the right paravertebral muscle. Panels **D** and **E**: liver volume calculated on hepatobiliary phase with free-hand contours using dedicated software (Intellispace Portal, Philips, The Netherlands).

**Table 2.** Demographic and clinical characteristics of study population

| Variables | Number (%) |
|---|---|
| Male gender | 186 (61.4) |
| Cirrhosis | 175 (57.8) |
| Radiologic cirrhosis | 116 (38.3) |
| Child–Pugh class | |
| A | 153 (81.8) |
| B | 24 (12.9) |
| C | 9 (4.8) |
| MELD | |
| ≤ 10 | 116 (64.1) |
| 11–18 | 64 (34.4) |
| 19–24 | 6 (3.3) |

sitivity and moderate specificity (66.7% and 53.8%), and with an AUROC of 0.617 (0.528–0.706 95% CI). On the contrary, the accuracy of irINTnorm in the assessment of liver function was very poor with an AUROC of 0.482 (0.381–0.583 95% CI) in discriminating Child–Pugh A vs. Child–Pugh B and C patients and an AUROC of 0.522 (0.426–0.617 95% CI) in discriminating MELD score ≤ 10 and > 10 (Fig. 5).

**Table 3.** Association between irHEPnorm and irINTnorm and cirrhosis, Child–Pugh class, and MELD class

| Variables | Mean (SD) | |
|---|---|---|
| | Enhancement hepatobiliary normalized | Enhancement interstitial normalized |
| Cirrhosis | | |
| No | | |
| 128 | 0.0005 (0.0003) | 0.0002 (0.0001) |
| Yes | | |
| 175 | 0.0004 (0.0002) | 0.0003 (0.0002) |
| *p* value | **0.010** | 0.060 |
| CHILD | | |
| A | | |
| 153 | 0.0004 (0.0002) | 0.0003 (0.0002) |
| B | | |
| 24 | 0.0003 (0.0002) | 0.0003 (0.0002) |
| C | | |
| 9 | 0.0002 (0.0002) | 0.0003 (0.0002) |
| *p* value | < **0.001** | 0.642 |
| MELD | | |
| ≤ 10 | | |
| 116 | 0.0004 (0.0002) | 0.0003 (0.0002) |
| 11–18 | | |
| 64 | 0.0003 (0.0002) | 0.0003 (0.0002) |
| 19–24 | | |
| 6 | 0.0003 (0.0003) | 0.0002 (0.0001) |
| *p* value | **0.018** | 0.902 |

Bold values are statistically significant ($p < 0.05$)

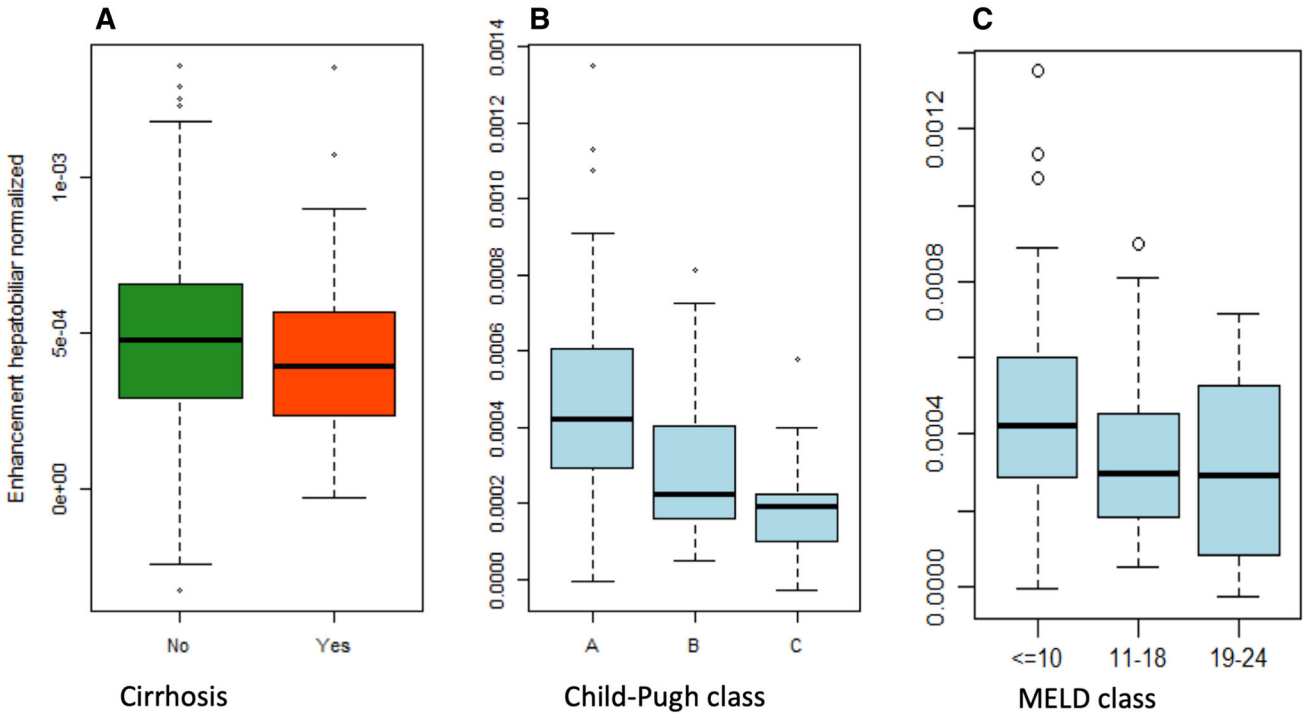


**Fig. 4.** Box plots showing the correlation between signal intensity of hepatobiliary phase normalized for liver volume and the presence of cirrhosis (**A**), Child–Pugh (**B**), and MELD class (**C**).

**Table 4.** Mean (± SD) of continuous variables

| Continuous variables | Mean (± SD) |
|---|---|
| Total bilirubin | 0.83 (0.58) |
| Direct bilirubin | 0.69 (0.45) |
| GOT | 37.77 (26.59) |
| GPT | 34.84 (27.53) |
| GGT | 68.93 (60.52) |
| ALP | 96.52 (47.58) |
| Sodium | 140.27 (2.81) |
| Albumin | 3.92 (0.61) |
| PT | 1.11 (0.14) |
| INR | 1.10 (0.14) |
| Creatinine | 0.90 (0.26) |
| MELD | 9.09 (3.95) |
| CHILD | 5.83 (1.40) |

## Discussion

The results of the present study showed that signal intensity normalized for LV in hepatobiliary phase was significantly lower in cirrhotic than non-cirrhotic patients, as expected, in line with the physiological assumption that cirrhosis is a dynamic process characterized by a progressive loss of hepatocyte function and a simultaneous increase of non-functioning fibrotic tissue. Moreover, comparing the signal intensity from interstitial to hepatobiliary phase in hepatopatic patients, we found a significant reduction of liver enhancement in comparison with control group. Alterations of hepatocytes, occurring in case of cirrhosis, led to a reduction of the expression of active carriers OATP1B1/B3, which are

**Table 5.** Association between irHEPnorm and irINTnorm and biochemical parameters, Child–Pugh score, and MELD score

| | Total bilirubin | GOT | GPT | GGT | ALP |
|---|---|---|---|---|---|
| Enhancement hepatobiliary normalized | − 0.258 (< 0.001) | **− 0.291 (< 0.001)** | **− 0.210 (< 0.001)** | **− 0.192 (0.002)** | **− 0.229 (< 0.001)** |
| Enhancement interstitial normalized | − 0.021 (0.733) | − 0.053 (0.382) | − 0.025 (0.666) | 0.033 (0.588) | − 0.07 (0.263) |
| | Sodium | Albumin | PT | INR | Creatinine |
| Enhancement hepatobiliary normalized | 0.026 (0.668) | **0.262 (< 0.001)** | **− 0.174 (0.007)** | **− 0.19 (0.002)** | − 0.011 (0.848) |
| Enhancement interstitial normalized | 0.017 (0.774) | − 0.003 (0.956) | 0.099 (0.130) | 0.066 (0.283) | 0.063 (0.284) |
| | | MELD | | | CHILD |
| Enhancement hepatobiliary normalized | | **− 0.192 (0.010)** | | | **− 0.292 (< 0.001)** |
| Enhancement interstitial normalized | | 0.092 (0.219) | | | 0.04 (0.588) |

Bold values are statistically significant ($p < 0.05$)

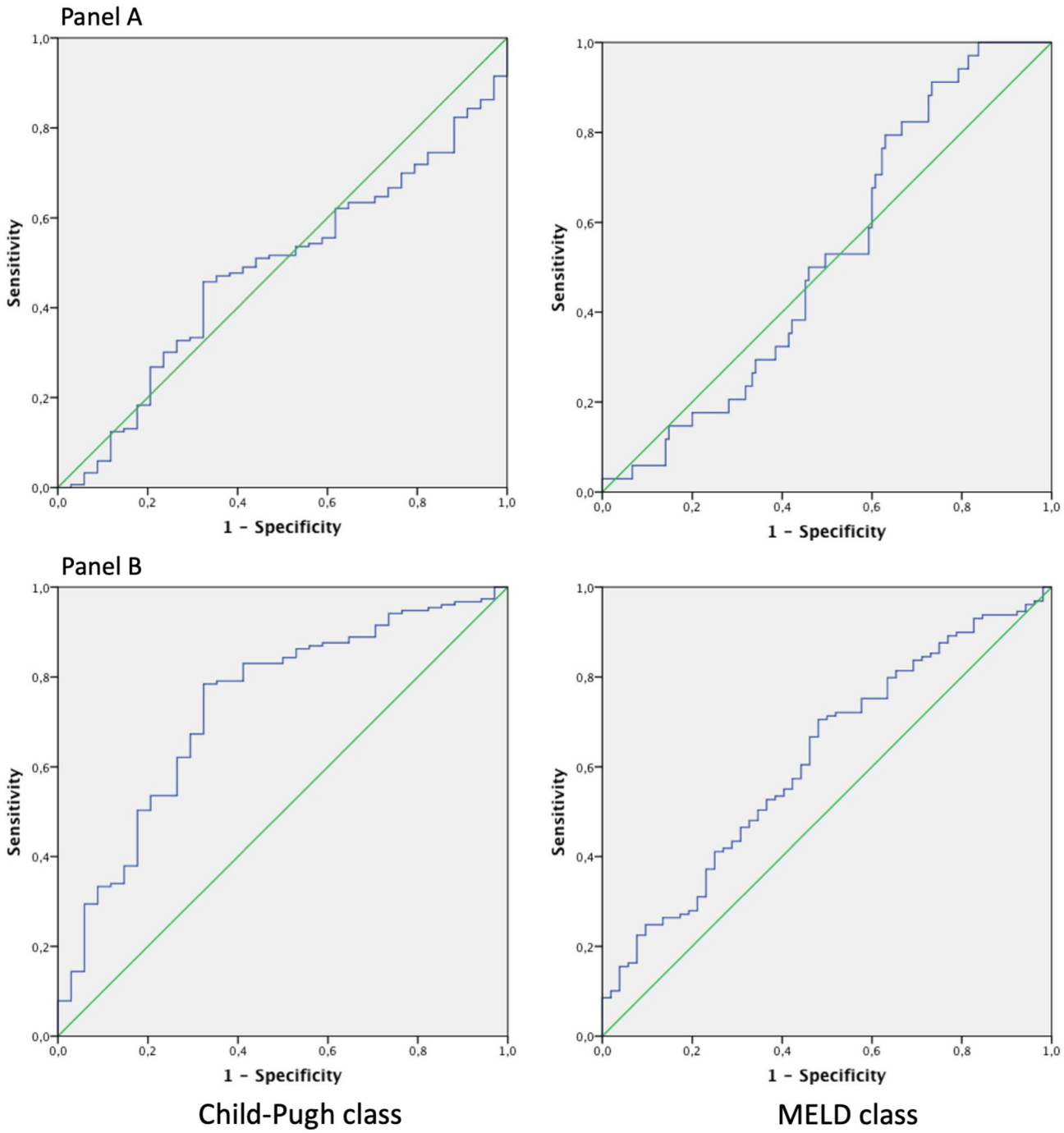


**Fig. 5.** ROC curves showing the ability of signal intensity of interstitial (panel **A**) and hepatobiliary (panel **B**) phase normalized for liver volume in discriminating Child–Pugh (class **A**, **B,** and **C**) and MELD class (≤ 10 and > 10).

located at the sinusoidal membrane, and are responsible not only for the uptake of Gd-EOB-DTPA but also of its excretion into the biliary system. Usually, the same carriers are involved in the uptake and excretion of bilirubin in liver cells and, indeed, it explains the relationship obtained between bilirubin biochemical serum levels and signal intensity variation in hepatobiliary phase.

In the last years, many authors attempted to demonstrate the relationship between Gd-EOB-DTPA-enhanced MRI studies and liver function by means of Child–Pugh [7, 8] and MELD scores [9], liver biopsy [10, 11], and ICG test [12, 13]. More recently, some researchers tried to correlate indexes of signal intensity normalized for liver volume, based on the assumption that both liver volume and function decrease with the progression of cirrhosis [14–16]. For all these purposes, several Gd-EOB-DTPA-enhanced MRI-based liver function indices have been used. Yoneyama et al. re-

ported that the relationship among seven different Gd-EOB-DTPA-enhanced MRI-based liver function indices and liver function expressed with ICG was stronger with LV ($r = -0.377$ to $-0.561$) than without ($r = -0.457$ to $-0.528$) [14]. Yamada et al. found out that the liver-to-spleen ratio multiplied for liver volume significantly correlated with ICG and that it could estimate segmental liver function, better than ICG and liver volume alone [16]. All these authors used ICG as expression of liver function. However, it has often been argued that ICG clearance is not a true liver function test, since it is blood-flow dependent and inaccurate in patients with cirrhosis because of decreased ICG extraction. Moreover, this technique is not available in every hepatobiliary surgical departments and may not be used in cases of regional dysfunction or heterogeneous distribution of functional and non-functional liver regions.

In line with previous published data, we observed a significant correlation between irHEPnorm and Child–Pugh score [7–9]. Indeed, previously, Tamada et al. found out that hepatic parenchymal enhancement decreased with the progression of cirrhosis; however, they failed in discriminating among Child–Pugh class, probably because signal intensity is not an absolute value and needs to be adjusted [7]. In our series, a correlation with MELD score, which is largely used in surgical departments to evaluate liver function and to address the more appropriate surgery, was found. As reported by other few published studies [9, 21], we obtained a significant association between MELD score and signal intensity of Gd-EOB-DTPA-enhanced MRI studies and we were able to demonstrate a progressive decrease of signal intensity in hepatobiliary phase, moving from patients with a better liver function (expressed as MELD score $\leq 10$) to a worse one (expressed as a MELD score $>19$).

Moreover, we identified two different cut-off values of signal intensity in hepatobiliary phase normalized for liver volume having good sensitivity and specificity in discriminating Child–Pugh class A from B and C patients (irHEPnorm = 0.262) and patients with MELD score $\leq 10$ and $> 10$ (irHEPnorm = 0.317).

The ability of irHEPnorm in differentiating among different liver function class categories, using definite cut-off values, can be added to other information as a complementary diagnostic tool for surgeons in the management of patients deemed suitable to surgery. In fact, the evaluation of candidates to hepatobiliary surgery is quite different from the evaluation of liver function in cirrhotic patients: in this setting, both the volume and condition of future remnant liver should be assessed to prevent post-hepatectomy liver failure.

This study has some limitations; first of all we used only one Gd-EOB-DTPA-enhanced MRI liver function index. In fact, we thought that the assessment of liver-to-muscle ratio was easier to perform, not representing a time-consuming option in comparison to all the other indexes already used in the literature.

Second, the sample of patients with poor liver function was relatively small. This is due to the improvement of screening follow-up of cirrhotic patients, which makes the enrolment of patients with decompensated liver function more difficult.

Lastly, only one radiologist performed ROI placements and so the reproducibility was not assessed. However, drawing the ROI as large as possible would avoid any possible heterogeneity.

In conclusion, our study suggests that the rate of liver-to-muscle ratio in hepatobiliary phase normalized for liver volume is a simple and reliable method that well correlates with liver function. These values can be easily calculated during Gd-EOB-DTPA-enhanced MRI studies and could be used in the pre-operative assessment of candidates to liver surgical, because by applying one single imaging technique we could provide both anatomical and functional information to guide surgeons in the choice of the more appropriate treatment.

**Acknowledgments** We would like to thank G. Querques for the extended revision of English grammar.

## References

1. Ünal E, Akata D, Karcaaltincaba M (2016) Liver function assessment by magnetic resonance imaging. Semin Ultrasound CT MR 37(6):549–560. https://doi.org/10.1053/j.sult.2016.08.006
2. Matsumata T, Kanematsu T, Yoshida Y, et al. (1987) The indocyanine green test enables prediction of postoperative complications after hepatic resection. World J Surg 11:678–681
3. Kwon A-H, Matsui Y, Ha-Kawa SK, Kamiyama Y (2001) Functional hepatic volume measured by technetium-99m-galactosyl-human serum albumin liver scintigraphy: comparison between hepatocyte volume and liver volume by computed tomography. Am J Gastroenterol 96:541. https://doi.org/10.1111/j.1572-0241.2001.03556.x
4. de Graaf W, Bennink RJ, Veteläinen R, van Gulik TM (2010) Nuclear imaging techniques for the assessment of hepatic function in liver surgery and transplantation. J Nucl Med 51:742–752. https://doi.org/10.2967/jnumed.109.069435
5. Tong C, Xu X, Liu C, Zhang T, Qu K (2012) Assessment of liver volume variation to evaluate liver function. Front Med 6(4):421–427. https://doi.org/10.1007/s11684-012-0223-5
6. Saygili OB, Tarhan NC, Yildirim T, et al. (2005) Value of computed tomography and magnetic resonance imaging for assessing severity of liver cirrhosis secondary to viral hepatitis. Eur J Radiol 54(3):400–407. https://doi.org/10.1016/j.ejrad.2004.08.001
7. Tamada T, Ito K, Higaki A, et al. (2011) Gd-EOB-DTPA-enhanced MR imaging: evaluation of hepatic enhancement effects in normal and cirrhotic livers. Eur J Radiol 80:311–316. https://doi.org/10.1016/j.ejrad.2011.01.020
8. Motosugi U, Ichikawa T, Sou H, et al. (2009) Liver parenchymal enhancement of hepatocyte-phase images in Gd-EOB-DTPA-enhanced MR imaging: which biological markers of the liver function affect the enhancement? J Magn Reson Imaging 30:1042–1046. https://doi.org/10.1002/jmri.21956
9. Verloh N, Haimerl M, Zeman F, et al. (2014) Assessing liver function by liver enhancement during the hepatobiliary phase with Gd-EOB-DTPA-enhanced MRI at 3 Tesla. Eur Radiol 24(5):1013–1019. https://doi.org/10.1007/s00330-014-3108-y
10. Nojiri S, Kusakabe A, Fujiwara K, et al. (2013) Noninvasive evaluation of hepatic fibrosis in hepatitis C virus-infected patients using ethoxybenzyl-magnetic resonance imaging. J Gastroenterol Hepatol 28(6):1032–1039. https://doi.org/10.1111/jgh.12181

11. Watanabe H, Kanematsu M, Goshima S, et al. (2011) Staging hepatic fibrosis: comparison of gadoxetate disodium-enhanced and diffusion-weighted MR imaging-preliminary observations. Radiology 259(1):142–150. https://doi.org/10.1148/radiol.10100621
12. Utsunomiya T, Shimada M, Hanaoka J, et al. (2012) Possible utility of MRI using Gd-EOB-DTPA for estimating liver functional reserve. J Gastroenterol 47:470–476. https://doi.org/10.1007/s00535-011-0513-8
13. Tajima T, Takao H, Akai H, et al. (2010) Relationship between liver function and liver signal intensity in hepatobiliary phase of gadolinium ethoxybenzyl diethylenetriamine pentaacetic acid-enhanced magnetic resonance imaging. J Comput Assist Tomogr 34(3):362–366. https://doi.org/10.1097/rct.0b013e3181cd3304
14. Yoneyama T, Fukukura Y, Kamimura K, et al. (2014) Efficacy of liver parenchymal enhancement and liver volume to standard liver volume ratio on Gd-EOB-DTPA-enhanced MRI for estimation of liver function. Eur Radiol 24:857. https://doi.org/10.1007/s00330-013-3086-5
15. Nishie A, Ushijima Y, Tajima T, et al. (2012) Quantitative analysis of liver function using superparamagnetic iron oxide- and Gd-EOB-DTPA-enhanced MRI: comparison with Technetium-99m galactosyl serum albumin scintigraphy. Eur J Radiol 81(6):1100–1104. https://doi.org/10.1016/j.ejrad.2011.02.053
16. Yamada A, Hara T, Li F, et al. (2011) Quantitative evaluation of liver function with use of gadoxetate disodium-enhanced MR imaging. Radiology 260:727–733. https://doi.org/10.1148/radiol.11100586
17. Karabulut N, Elmas N (2006) Contrast agents used in MR imaging of the liver. Diagn Interv Radiol. 12(1):22–30
18. European Association for Study of Liver, Asociacion Latinoamericana para el Estudio del Higado (2015) EASL-ALEH Clinical Practice Guidelines: non-invasive tests for evaluation of liver disease severity and prognosis. J Hepatol 63(1):237–264. https://doi.org/10.1016/j.jhep.2015.04.006
19. Pugh RN, Murray-Lyon IM, Dawson JL, Pietroni MC, Williams R (1973) Transection of the oesophagus for bleeding oesophageal varices. Br J Surg 60:646–649
20. Wiesner R, Edwards E, Freeman R, et al. (2003) Model for end-stage liver disease (MELD) and allocation of donor livers. Gastroenterology 124(1):91–96. https://doi.org/10.1053/gast.2003.50016
21. Chernyak V, Kim J, Rozenblit AM, Mazzoriol F, Ricci Z (2011) Hepatic enhancement during the hepatobiliary phase after gadoxetate disodium administration in patients with chronic liver disease: the role of laboratory factors. J Magn Reson Imaging 34(2):301–309. https://doi.org/10.1002/jmri.22635